online data

Agonist-induced regulation of mitochondrial and endoplasmic reticulum motility

David BROUGH, Michael J. SCHELL and Robin F. IRVINE[1]

Department of Pharmacology, University of Cambridge, Tennis Court Road, Cambridge CB2 1PD, U.K.

Using fluorescently tagged markers for organelles in conjunction with confocal microscopy, we have studied the effects of agonist-induced Ca^{2+} signals on the motility of mitochondria and the ER (endoplasmic reticulum). We observed that the muscarinic agonist carbachol produced a rapid, simultaneous and reversible cessation of the movements of both organelles, which was dependent on a rise in cytosolic Ca^{2+}. This rise in Ca^{2+} was shown to cause a fall in cellular ATP levels, and the effect of carbachol on organelle movement could be mimicked by depleting ATP with metabolic inhibitors in the absence of any such rise in Ca^{2+}. However, a Ca^{2+}-sensing process independent of ATP appears also to be involved, because we identified conditions where the ATP depletion was blocked (by inhibitors of the Ca^{2+} pumps), but the organelle movements still ceased following a rise in cytosolic Ca^{2+}. We conclude that the co-ordinated cessation of mitochondria and ER motility is a process regulated by the cytosolic concentration of both Ca^{2+} and ATP, and that these two parameters are likely to synergize to regulate the localization of the two organelles, and to facilitate the transfer of Ca^{2+} between them.

Key words: ATP, calcium signalling, endoplasmic reticulum, mitochondria, organelle movement.

INTRODUCTION

Complex spatial and temporal calcium (Ca^{2+}) signals activate a variety of cellular responses. Cells regulate Ca^{2+} signalling patterns in part through the localization of the ER (endoplasmic reticulum) and the mitochondria, organelles that buffer and store cytosolic Ca^{2+}. Mitochondria are often found localized very close to Ca^{2+}-release channels on the ER and plasma membrane. Such 'hotspots' are microdomains of high local [Ca^{2+}], which allow released Ca^{2+} to be sensed by the electrogenic mitochondrial Ca^{2+}-uniporter, resulting in Ca^{2+} sequestration in mitochondria [1]. The sequestration and subsequent transfer of Ca^{2+} back to the ER influences processes such as ER Ca^{2+}-store refilling and CCE (capacitative Ca^{2+} entry) [2]. Furthermore, in pancreatic acinar cells the mitochondria form a 'belt' surrounding the apical domain, confining IP_3 (inositol 1,4,5-trisphosphate)-generated Ca^{2+} spikes to this region [3]. In HeLa cells, mitochondrial uptake of Ca^{2+} is determined in part by the nature of the Ca^{2+} signal, and IP_3-generated Ca^{2+} is taken up preferentially compared with Ca^{2+} entering the cytosol from other sources [4]. These and other examples (e.g. see [5]) demonstrate that the spatial relationship between the ER and mitochondria is a critical determinant of complex cytosolic Ca^{2+} signals.

This special relationship can also act reciprocally, whereby Ca^{2+} signals regulate organelle dynamics [6,7]. Both ER and mitochondria are highly motile within cells. The fluorescent carbocyanine dye $DiOC_6(3)$ (3,3′-dihexyloxacarbocyanine) first allowed the visualization of multiple forms of ER movement [8,9]. The movement of ER tubules is known to depend largely upon the microtubule framework, with a significant proportion of detectable ER movement reflecting microtubule dynamics and plus-end-directed motor transport [10]. Mitochondrial transport/movement also occurs along the microtubule framework, powered by the molecular motor proteins kinesin and cytoplasmic dynein, with the actin cytoskeleton also involved [11–13]. Glutamate-induced cytosolic Ca^{2+} increases were shown to inhibit mitochondrial mobility in neurons, and this was suggested to occur as a result of ATP depletion, since the uncoupler FCCP (carbonyl cyanide *p*-trifluoromethoxyphenylhydrazone) exhibited the same effect [6]. In cultured hippocampal neurons, mitochondria are known to localize, as might be expected, in areas of high ATP demand, such as the synapses [14]. The mechanism by which this occurs remains to be determined, although association with docking proteins is one possibility [13]. A recent paper defines a possible homoeostatic mechanism of Ca^{2+} feedback, regulating mobility and localization of mitochondria [7].

In the present paper we have used a simple method to analyse the movement of intracellular organelles, and thus to investigate the effects of large cytosolic Ca^{2+} signals on the mobility of ER and mitochondria simultaneously. We observe that either the ATP depletion or the Ca^{2+} signal induced by an agonist can halt organelle movement, and that the two processes probably co-operate to arrest organelle movement near hotspots of Ca^{2+} signalling activity. Our results suggest a mechanism whereby mitochondria might be localized near microdomains of high Ca^{2+} load in order to generate ATP near areas of high energy demand, and also Ca^{2+} transfer between mitochondria and ER may be facilitated.

EXPERIMENTAL

Materials

HEK-293 cells stably expressing ER-targeted GFP (green fluorescent protein) [15] were kindly given by Dr G. St. J. Bird (NIEHS, Research Triangle Park, NC, U.S.A.). The construct

Abbreviations used: AM, acetoxymethyl ester; BAPTA/AM, bis-(*o*-aminophenoxy)ethane-*N,N,N′,N′*-tetra-acetic acid tetrakis(acetoxymethyl ester); $[Ca^{2+}]_i$, cytosolic Ca^{2+} concentration; CCCP, carbonyl cyanide *m*-chlorophenylhydrazone; CCh, carbachol; DMEM, Dulbecco's modified Eagle's medium; 2-DOG, 2-deoxyglucose; ER, endoplasmic reticulum; FBS, foetal bovine serum; FCCP, carbonyl cyanide *p*-trifluoromethoxyphenylhydrazone; GFP, green fluorescent protein; IP_3, inositol 1,4,5-trisphosphate; MI, mobility index; PMCA, plasma-membrane Ca^{2+}-ATPase; WT, wild-type.

[1] To whom correspondence should be addressed (email rfi20@cam.ac.uk).

for expressing firefly luciferase in the cytosol (pGL3-control) was purchased from Promega. The expression vector targeting DsRed to the mitochondria, using the mitochondrial targeting sequence from cytochrome *c* oxidase (pDsRed1-Mito), was purchased from ClonTech. Fura Red/AM (acetoxymethyl ester) and Mitotracker Red were purchased from Molecular Probes. DMEM (Dulbecco's modified Eagle's medium), FBS (foetal bovine serum), L-glutamine and penicillin/streptomycin were supplied by Life Technologies. All other reagents were supplied by Sigma. CCh (carbachol) was used where indicated at 100 μM, and was prepared as a 10 mM stock in imaging buffer (in mM: 121 NaCl, 5.4 KCl, 0.8 $MgCl_2$, 1.8 $CaCl_2$, 6 $NaHCO_3$, 5.5 glucose, 25 Hepes/NaOH, pH 7.3) [16]. All treatments were bolus-applied to the imaging chamber. Imaging buffer containing low calcium was prepared as described above, except for the omission of $CaCl_2$ and the addition of 2 mM EGTA.

For some experiments, the cells were incubated in a buffer containing 1 mM Gd^{3+} to insulate the plasma membrane from Ca^{2+} fluxes (see [17] for a full explanation of the rationale and characterization of this technique). The buffer used was the same as in [17], which is, in mM: 120 NaCl, 5.4 KCl, 0.8 Mg_2SO_4, 1.8 $CaCl_2$, 10 glucose, 1 $GdCl_3$, 20 Hepes/NaOH, pH 7.4.

Cell culture and transfection

WT (wild-type) and stably transfected HEK-293 cells were passaged and maintained in DMEM [containing 10 % (v/v) FBS, 5 mM glutamine, 50 units/ml penicillin and 50 units/ml streptomycin] at 37 °C in an atmosphere of 5 % CO_2. Two days before experimentation, the cells were seeded on to 25 mm glass coverslips (Menzel-Glaser, Braunschweig, Germany) coated with poly(D-lysine). Cells were seeded at a density of 0.5×10^6 cells/ml and incubated overnight (37 °C in an atmosphere of 5 % CO_2). At 1 h before transfection, the cells were washed with fresh medium. pDsRed1-Mito was transfected into cells using FuGENE™ 6 Transfection reagent (Roche). pDsRed1-Mito-expressing cells were examined 24 h post-transfection.

Organelle imaging

Stably transfected HEK-293 cells were plated on to coated glass coverslips to the stated density (37 °C, 5 % CO_2). Initially, the coverslips were incubated with 50 nM Mitotracker Red (Molecular Probes, Eugene, OR, U.S.A.) for 10 min, before the coverslip was mounted into an imaging chamber and immersed with 1 ml of imaging buffer. The imaging chamber was placed on to the heated stage of a Zeiss LSM 510 microscope. All movement experiments were conducted at 37 °C. GFP and Mitotracker Red were excited with 488 nm and 543 nm lines of argon and helium/neon lasers respectively. GFP fluorescence emission was collected through a 505–530 nm filter and Mitotracker Red fluorescence emission was collected through a 560 nm long-pass filter. ER and mitochondrial 512×512 pixel resolution images were collected simultaneously every 3.15 s. Following the collection of enough frames to establish a baseline for subsequent analysis (usually approx. 50 frames), either vehicle (10 μl imaging buffer) or CCh (100 μM) were bolus-applied to the imaging chamber. Images were then continued to be collected for at least 50 frames, or until the end of the experiment. Where indicated, experiments were performed in low Ca^{2+} imaging buffer, and the bolus addition of 2 mM free Ca^{2+} is also shown.

Involvement of ATP

The protocol used was as described above, except for the following exceptions: cells expressing pDsRed1-Mito were used because mitochondrial depolarization with the protonophore CCCP (carbonyl cyanide *m*-chlorophenylhydrazone) resulted in a loss of Mitotracker Red from the mitochondria. Following the collection of approx. 30 confocal images, the following combinations of metabolic poisons were applied: 5 mM 2-DOG (2-deoxyglucose); 5 mM 2-DOG and 1 μM CCCP; or 15 mM 2-DOG and 1 μM CCCP. A further series of confocal images were collected to allow assessment of organelle movement before the addition of 100 μM CCh.

Analysis of movement

The method of movement analysis described here involves plotting the mean fluorescence intensities of a subtracted image series, and is in principle similar to analyses described elsewhere [6]. Essentially, a confocal time series, consisting of a stack of frames, was opened using ImageJ software (http://rsb.info.nih.gov/ij/). Using the slice-to-slice difference macro, pixel intensities (measured in units of grey value) in each frame were subtracted from the next frame in series so that only the difference in pixel intensity remained. Thus, in the absence of movement, subtraction of one frame from another would result in a value of zero. The macro employed records only positive changes in pixel intensity between images, negative values being automatically converted into zero. This method therefore results in the measurement of one 'movement event' for each movement of organelle between frames. To control for changes in cell shape/volume that may affect the fluorescence intensities and therefore our analysis of organelle movement, data are normalized as the ratio of subtracted fluorescence values over non-subtracted. This parameter is referred to throughout as the MI (mobility index).

Calcium imaging

Changes in $[Ca^{2+}]_i$ (cytosolic Ca^{2+} concentration) were measured using the calcium indicator Fura Red, whose fluorescence emission decreases upon binding calcium. Cells on coated glass coverslips were loaded for 20 min at 37 °C with 5 μM Fura Red/AM (Molecular Probes) dissolved in DMSO. Excess Fura Red was washed from the cells with pre-warmed imaging buffer. The coverslip was mounted into an imaging chamber, immersed with 1 ml of imaging buffer and imaged as described for organelle movement. The 488 nm line of the argon laser was used to excite Fura Red, and fluorescence emission was collected through a long-pass 585 nm filter.

For experiments investigating the effects of ATP depletion and Gd^{3+} insulation on $[Ca^{2+}]_i$, WT HEK-293 cells were seeded into a 96-well plate at a density of 5×10^4 cells/well. Cells were loaded with 2 μM Fluo-4/AM for 40 min. Before experimentation, the cells were immersed in 100 μl of the appropriate buffer per well. The plate was mounted in a fluorescence spectrometer, FlexStation™ (Molecular Devices, Sunnyvale, CA, U.S.A.), which collected fluorescence output from each well, with data acquired at 2 s intervals. Any agonists or drugs were added to the well in a 50 μl volume 30 s after the start of fluorescence recording. Fluo-4 was excited at 485 nm, with fluorescence emission collected at 520 nm. The wells were imaged for 10 min at room temperature ($\approx$ 18 °C).

Bioluminescence measurements

HEK-293 cells were seeded in a 75 cm^2 flask and grown to 75 % confluence. The medium was changed 1 h before transfection with pGL3-control vector (Promega) using the calcium phosphate method [18]. The pGL3-control contains a modified version of the

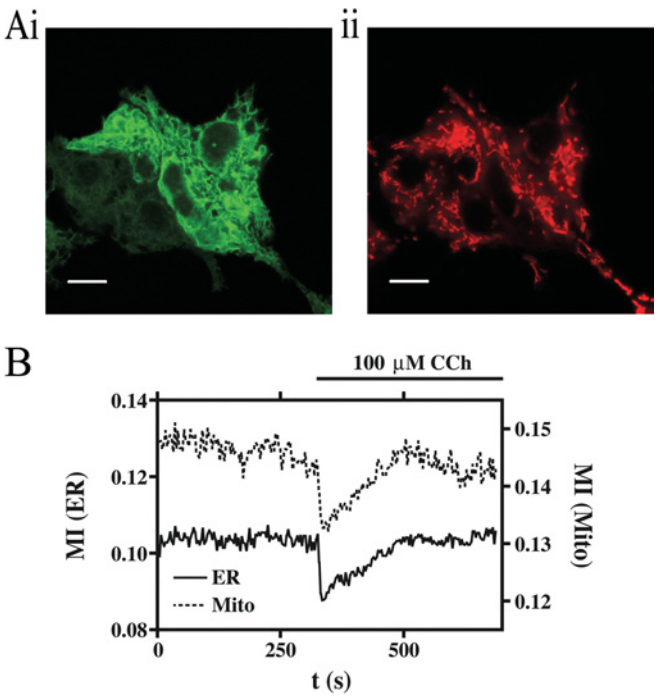

Figure 1 The effects of 100 μM carbachol (CCh) on organelle mobility

(**A**) HEK-293 cells stably expressing GFP targeted to the ER (**i**) and loaded with Mitotracker Red (**ii**) illustrate the respective organelle morphology and distribution. Scale bar represents a distance of 10 μm. (**B**) The change in organelle mobility, described here as the MI, following the addition of CCh for both the ER (continuous line) and mitochondria (Mito; broken line). See Supplementary Movie 1 (http://www.BiochemJ.org/bj/392/bj3920291add.htm for a full version of this Figure.

firefly (*Phontinus pyralis*) luciferase gene providing constitutive cytosolic expression [19]. At 24 h following transfection, the cells were trypsin-treated, spun (80 ***g*** for 5 min in a Jouan C 312 centrifuge; Jouan, Newport Pagnell, Bucks., U.K.) and resuspended in 1 ml of imaging buffer. The cell suspension was diluted 1:5 with imaging buffer and incubated with 500 μM D-luciferin (Europa Bioproducts Ltd., Ely, Cambs., U.K.) for at least 15 min. An aliquot (1 ml) of cell suspension was then transferred to a luminescence tube and loaded into the luminometer housing. Bioluminescence was continuously measured (with a 1 s integration time) by a photomultiplier tube (PMT 9899A; Electron Tubes, Ruislip, London, U.K.). Bioluminescence experiments were conducted at room temperature.

Data presentation

All mobility and calcium traces are representative of at least six separate experiments.

RESULTS

We utilized confocal microscopy to collect simultaneously fluorescent images of living HEK-293 cells stably expressing ER-targeted GFP and loaded with Mitotracker Red (Figure 1Ai and ii). For each experiment, the observation of organelle movement lasted no less than 5 min. Following the addition of a supramaximal dose (100 μM) of the muscarinic receptor agonist CCh, we observed an inhibition of organelle mobility similar to that which has been described recently for mitochondria [7] (see Supplementary Movie 1; http://www.BiochemJ.org/bj/392/bj3920291add.htm); that is, both the ER and mitochondria show an inhibition that is transient and recovers over several minutes. This response is clearly visible in the movie, and can be recorded using the analysis that we describe in the Experimental section (Figure 1B). The movement of mitochondria was initially followed by Mitotracker Red, as shown in Figure 1. However, in later experiments, when we used drugs that interfere with mitochondrial function such as CCCP, we turned to transfecting the cells transiently with mitochondrially targeted DsRed (see the Experimental section) so as to avoid any artefacts caused by changes in mitochondrial activity or membrane potential. We repeated all the main observations, such as the effect of CCh or thapsigargin with DsRed-transfected cells, and found no difference from Mitotracker Red (results not shown). Moreover, the absence of any signal, or change of signal, in the red wavelength in untransfected cells (adjacent to those transfected with DsRed) shows that there is no significant autofluorescence (for example, from NADH/FAD) to complicate our analysis of mitochondrial movement.

Using calcium imaging, we determined that, in these experiments, the GFP-expressing HEK-293 cells responded to CCh with a large initial $[Ca^{2+}]_i$ signal followed by a pattern of oscillations (Figure 2A). Correlation of organelle mobility with intracellular Ca^{2+} dynamics established that the transient inhibition occurred just after the initial Ca^{2+} response, but that no further inhibitions were evident during the repeated Ca^{2+} oscillations that followed (Figure 2A). This is in contrast with a recent report that showed that repeated inhibitions in mitochondrial mobility occurred in step with repeated cytosolic Ca^{2+} transients in H9c2 myoblasts [7]; we assume that, in the latter cells, either the $[Ca^{2+}]_i$ oscillations were greater, or the response was more sensitive to changes in $[Ca^{2+}]_i$. Evidence for the involvement of increased $[Ca^{2+}]_i$ in the inhibition of organelle mobility is shown in Figure 2(B) where, under conditions of low extracellular Ca^{2+}, both the challenge by CCh and the subsequent addition of Ca^{2+} to the bath solution resulted in transient inhibitions of both ER and mitochondrial mobility. Moreover, pre-incubation of the cells (for 25 min) with the Ca^{2+} chelator, BAPTA/AM [bis-(*o*-aminophenoxy)ethane-*N*,*N*,*N*′,*N*′-tetra-acetic acid tetrakis(acetoxymethyl ester); 20 μM], completely abolished the effects of CCh on ER and mitochondrial mobility (Figure 2C), illustrating the absolute dependence of this effect on the increase in $[Ca^{2+}]_i$.

We considered whether the inhibition of organelle mobility was a direct effect of increased $[Ca^{2+}]_i$, as suggested recently [7], or rather occurred as a consequence of some more remote process downstream from the Ca^{2+} signal. For example, it has been reported that stimulation of HeLa cells with a supramaximal histamine concentration causes a transient depletion of both cytosolic and mitochondrial ATP, largely as a consequence of increased Ca^{2+}-ATPase activity [20]. Similarly, in our system, triggering a large $[Ca^{2+}]_i$ signal might result in a transient fall in ATP levels, in part due to such an increased Ca^{2+}-ATPase activity. There might also be a contribution from a transient depolarization of the inner mitochondrial membrane inhibiting ATP production by oxidative phosphorylation. Whatever the cause, the depletion of cellular ATP could cause the motor proteins driving organelle mobility to stop, until ATP levels recover.

Thus we tested various interventions designed to cause directly transient or more permanent depletions of cellular ATP, and determined their effects on organelle mobility. The addition of 5 mM 2-DOG resulted in a transient inhibition of ER and mitochondrial mobility that recovered and was sensitive to subsequent CCh challenge (Figure 3Ai). Co-addition of 1 μM CCCP with 5 mM 2-DOG resulted in a more sustained inhibition of mitochondrial mobility (Figure 3Aii). The most severe intervention tested to

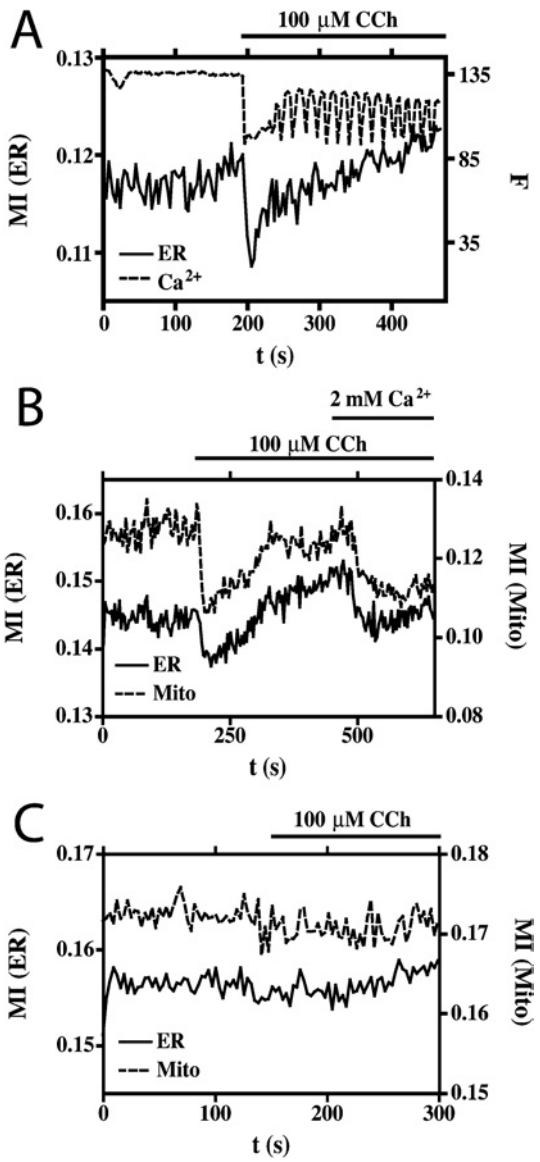

Figure 2 Ca^{2+}-dependence of inhibited organelle movement

(**A**) Correlation of $[Ca^{2+}]_i$ with ER mobility in response to CCh. The change in $[Ca^{2+}]_i$ is recorded as a change in Fura Red fluorescence (broken line), and is expressed in arbitrary units. Effects on ER mobility (continuous line) are expressed as the change in MI. (**B**) The change in ER (continuous line) and mitochondrial (Mito; broken line) mobility in response to CCh, and addition of Ca^{2+} to the bathing solution under conditions of low extracellular Ca^{2+}, followed by re-addition of Ca^{2+}. (**C**) The effects of CCh on ER (continuous line) and mitochondrial (broken line) mobility in cells pre-incubated with the Ca^{2+}-chelator BAPTA/AM under conditions of normal extracellular Ca^{2+}.

inhibit organelle mobility, 15 mM 2-DOG and 1 μM CCCP, resulted in an even more sustained inhibition; however, this did recover, and in the case of the ER, was sensitive to subsequent challenge with CCh (Figure 3Aiii). These data are consistent with a model whereby the cessation of organelle motility could be due to ATP depletion.

To gain more evidence to test this idea, we directly measured the effect of the agonists/inhibitors on [ATP]. HEK-293 cells expressing cytosol-targeted firefly luciferase, bathed in 500 μM D-luciferin (see the Experimental section), allowed us to measure the ATP dynamics in living cells. Following addition of CCh into the luminescence chamber, a fall in bioluminescence was observed, indicating a fall in [ATP] (Figure 3B), as previously shown by Jouaville et al. [20]. Following this depletion, there was a recovery in [ATP], to an enhanced baseline, before the addition of 15 mM 2-DOG and 1 μM CCCP resulted in a sustained depletion. Interestingly, the mobility of both the ER and the mitochondria recover, even in the presence of 15 mM 2-DOG and 1 μM CCCP (Figures 3Aiii and 3Aiv), although this reversibility was not reflected by the bioluminescence experiment (Figure 3B). The explanation for this probably lies in the relative affinities for ATP of these systems: *in vitro*, firefly luciferase has a reported affinity for ATP of 400 μM [21] (although in a 'cytosol-like' buffer the affinity is reported to decrease to a K_m value close to 2 mM [22]). The microtubule-based molecular motors, however, have higher ATP affinities [23], and may therefore respond to ATP when it recovers to a new (reduced) baseline at which luciferase is inactive, and at which we therefore cannot detect the ATP recovery.

One possible consequence of ATP depletion by the interventions described (Figure 3) could be an unopposed Ca^{2+} leak from the ER store, leading to a rise in $[Ca^{2+}]_i$. If that were so, it could be the Ca^{2+} rise, rather than the ATP drop, that was causing the cessation of organelle movement. However, the addition of 5 mM 2-DOG had no effect on $[Ca^{2+}]_i$, and the other interventions (5 mM 2-DOG and 1 μM CCCP, and 15 mM 2-DOG and 1 μM CCCP) induced only a moderate increase in $[Ca^{2+}]_i$ (Figure 4B), possibly due to mitochondrial Ca^{2+} release following their depolarization. These data therefore suggest that a transient depletion in cellular [ATP] can inhibit organelle mobility independently of any changes in $[Ca^{2+}]_i$.

This conclusion then raises a hypothesis contrary to that of Yi et al. [7]; that is, perhaps none of the effects of Ca^{2+} on organelle movement are direct, but are all caused by a drop in ATP engendered by increased activity of Ca^{2+}-ATP pumps in the ER and plasma membrane [20,24]. To test this, we employed (see the Experimental section) a recently described strategy (which also used HEK-293 cells), whereby bathing the cells in an extracellular buffer containing 1 mM Gd^{3+} 'insulates' the plasma membrane, and prevents Ca^{2+} entry and extrusion from the cytosol [17]. This treatment also prevents activation of the PMCA (plasma-membrane Ca^{2+}-ATPase), so the addition of thapsigargin should raise $[Ca^{2+}]_i$ with only a small (or even no) effect on [ATP].

Incubation of HEK-293 cells under such Gd^{3+}-insulating conditions (Figure 5) had the expected effect on the $[Ca^{2+}]_i$ response to CCh in that, following the cytosolic Ca^{2+} peak in response to CCh, there was a slightly more sustained phase of elevated $[Ca^{2+}]_i$ (Figure 5A) compared with the response under Gd^{3+}-free conditions (Figure 4A), although CCh still gave its now characteristic transient inhibitory effect on organelle mobility (Figure 5Ci). However, as described previously [17], the response of the cells to thapsigargin under conditions of Gd^{3+} insulation was dramatic, because the unopposed Ca^{2+} leak from the ER could no longer be controlled by the PMCA; the result was a sustained, elevated level of $[Ca^{2+}]_i$ for the duration of the experiment (Figure 5A). The effects on organelle mobility were equally marked, as the addition of thapsigargin under conditions of Gd^{3+} insulation resulted in the sustained cessation of mitochondrial and ER mobility (Figure 5Cii, and Supplementary Movie 2; http://www.BiochemJ.org/bj/392/bj3920291add.htm).

When we then measured [ATP] directly in this protocol, we confirmed that the addition of thapsigargin did not deplete cellular [ATP]; in fact, it actually caused a modestly enhanced level (Figure 5B), perhaps due to Ca^{2+}-stimulated mitochondrial metabolism. Thus we have clear evidence suggesting that a depletion of ATP in the absence of a rise in Ca^{2+} (Figures 3 and 4), and a Ca^{2+} rise in the absence of ATP depletion (Figure 5),

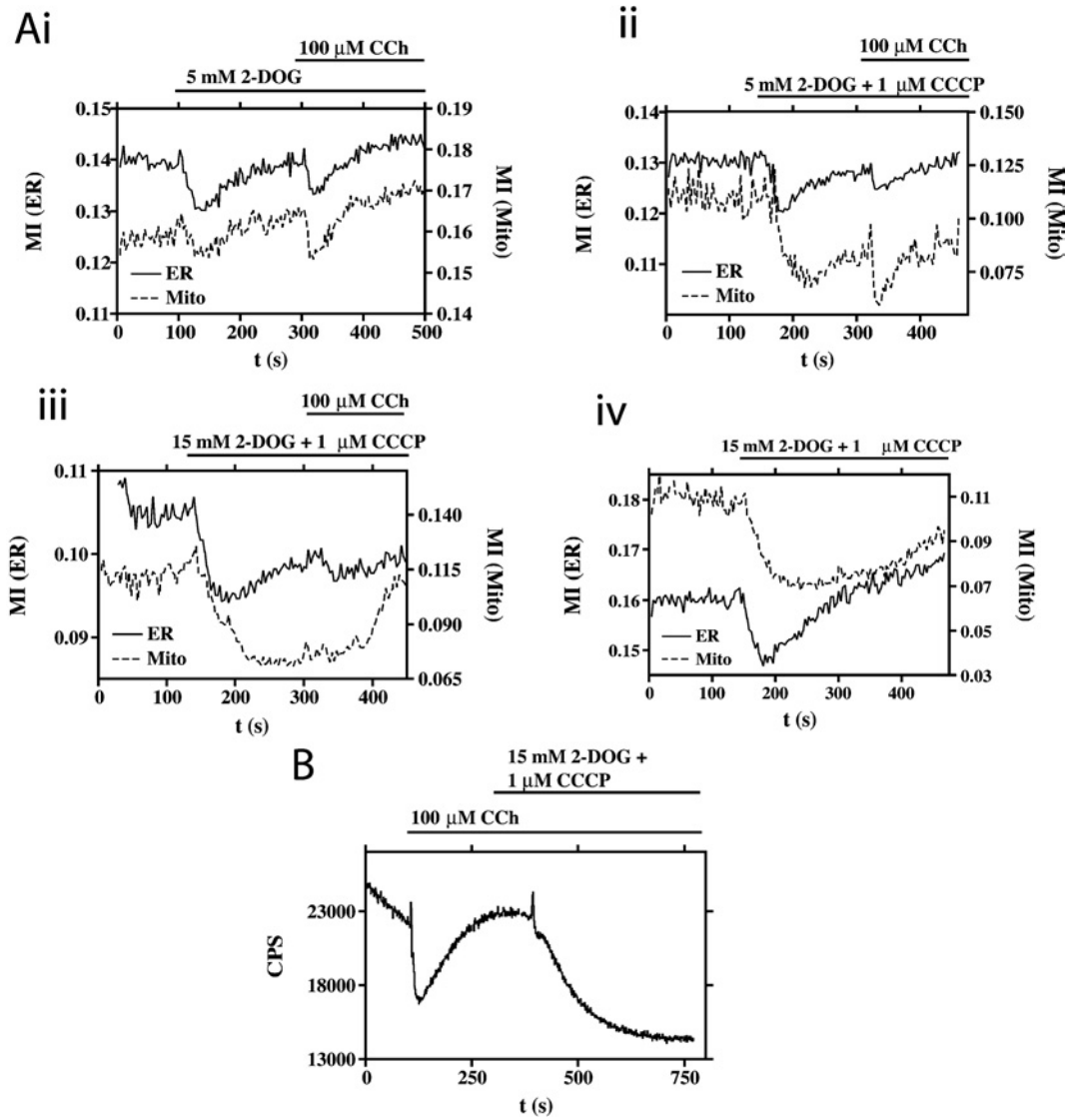

Figure 3 Dependence of organelle movement on [ATP]

(**A**) The effects of interventions (combinations of 2-DOG and CCCP) designed to have a transient (**i**, **ii**) or permanent (**iii**, **iv**) effect on cellular [ATP] in relation to ER (continuous line) and mitochondrial (Mito; broken line) mobility. (**B**) Effects of CCh and metabolic inhibitors on [ATP]. HEK-293 cells transiently expressing cytosol-targeted firefly luciferase, bathed in D-luciferin, stimulated with CCh followed by an intervention designed to permanently reduce cellular [ATP] (see above and the main text for further details). Bioluminescence is expressed as counts/second (CPS).

can both cause a simultaneous cessation of ER and mitochondrial movement.

DISCUSSION

In these experiments we have uniquely followed the movement of mitochondria and ER simultaneously in the same cell. We find evidence that either an increase in $[Ca^{2+}]_i$ or a depletion in [ATP] can inhibit the movement of these organelles, and within the limits of our quantification we found no condition where the movement properties of these two organelle types could be separated. The similar kinetic profiles of movement inhibition suggest a common mechanism of organelle movement regulation.

Our study extends the recently proposed hypothesis of a 'homoeostatic circuit', where Ca^{2+} inhibition of mitochondrial movement is suggested as a mechanism to enhance the mitochondrial Ca^{2+} signal [7]. In this model, the cessation of mitochondrial movement near sites of high calcium helps to facilitate the transfer of Ca^{2+} taken up into mitochondria back into the ER. Such a mechanism would function most efficiently if not only the donor organelle (mitochondria) but also the recipient organelle (ER) ceased movement. We have found that this is so, and our data suggest that such a mechanism would also allow both the ER and mitochondria (and possibly other microtubule-based cargoes) to localize preferentially to areas of high Ca^{2+} or low ATP, or both.

Movement of organelles along the microtubule framework involves motor proteins, which are ATPases. Thus [ATP] depletion in response to a CCh-induced $[Ca^{2+}]_i$ rise [20], which we have confirmed (Figure 3), might be a sufficient explanation for organelles ceasing to move. However, our data also support an additional hypothesis involving a Ca^{2+} sensor, which interacts with the motor machinery, as suggested in [7]. Another possibility is that Ca^{2+} is actually promoting tethering of mitochondria, and thus inhibiting

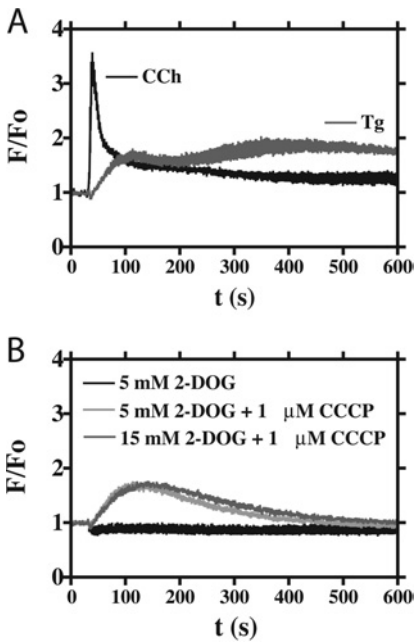

Figure 4 Effects of ATP depletion on $[Ca^{2+}]_i$

(**A**) WT HEK-293 cells were loaded with Fluo-4/AM and stimulated with either 100 μM CCh or 1 μM thapsigargin (Tg). The black trace represents the mean CCh response (four replicates), and the grey trace represents the mean thapsigargin response (four replicates). The data are presented as F/F_0. (**B**) WT HEK-293 cells were loaded with Fluo-4/AM and stimulated with interventions (combinations of 2-DOG and CCCP) designed to have transient or permanent effects on cellular [ATP] (cf. Figure 3). The key featured as an inset indicates the treatments applied. The data represent the means of four replicates, and are shown as F/F_0.

their Brownian motion, though the effect of ATP depletion would probably argue against this explanation. Whatever the mechanism, in situations of elevated $[Ca^{2+}]_i$ a period of ATP consumption due to increased Ca^{2+} pumping will occur prior to mitochondrial Ca^{2+} uptake and the activation of Ca^{2+}-sensitive mitochondrial dehydrogenases [20,25]. We propose that this depletion of ATP could synergize with the rise in $[Ca^{2+}]_i$ to reduce organelle movement.

Finally, although our experiments were performed in HEK-293 cells, the mechanisms we have uncovered may help to control the mitochondrial distribution in neurons. Both anterograde and retrograde mitochondrial movement along axons has been reported [26], with localization occurring in areas of high ATP demand, such as the growth cone of an extending axon [27]. A recent study analysed movement of mitochondria into the dendrites of hippocampal neurons undergoing electrical stimulation [28]. Mitochondria were found to move into these areas of intense energy requirement, a move that was inhibited by the NMDA (*N*-methyl-D-aspartate) receptor antagonist APV (D,L-2-amino-5-phosphonovaleric acid). Inhibition of mitochondrial movement was also reported in neurons following glutamate treatment, with the effect mimicked by the uncoupler FCCP [6]. Glutamate activation of neurons will induce a rise in Ca^{2+} as well as a fall in ATP, and the mechanisms described above may combine to provide an additive effect on mitochondrial localization, such that pathological levels of ATP depletion or $[Ca^{2+}]_i$ are not required. The consequences of such mechanisms would be to accumulate mitochondria near sites of intense metabolic and synaptic activity – and to allow the efficient transfer of the large quantities of cytosolic Ca^{2+} appearing during synaptic activity to be rapidly and transiently sequestered in mitochondria, and then transferred to the ER.

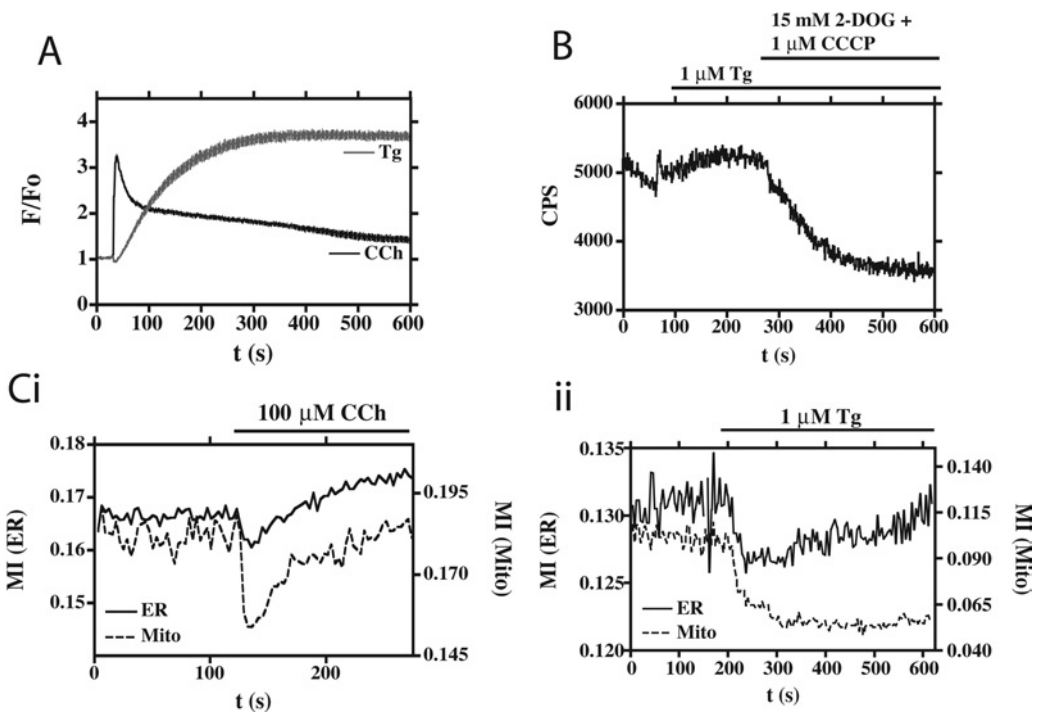

Figure 5 Organelle movement, [ATP] and $[Ca^{2+}]_i$ in cells incubated with 1 mM Gd^{3+}

The effects of 100 μM CCh (black trace) and 1 μM thapsigargin (Tg; grey trace) on $[Ca^{2+}]_i$ in WT HEK-293 cells loaded with Fluo-4/AM. Data are the means of nine replicates, and are represented as F/F_0. (**B**) Effects of Tg on [ATP]. HEK-293 cells transiently expressing cytosol-targeted firefly luciferase were bathed in D-luciferin and stimulated with Tg, followed by an intervention designed to permanently reduce cellular [ATP]. Bioluminescence is expressed as counts/second (CPS). (**C**) The mobility of the ER and the mitochondria. HEK-293 cells stably expressing GFP targeted to the ER, co-expressing mitochondrially targeted DsRed, were stimulated with either CCh (**i**) or Tg (**ii**). Mobility, expressed as the MI, is shown for the ER (continuous line) and mitochondria (broken line) respectively. Also see Supplementary Movie 2 (http://www.BiochemJ.org/bj/392/bj3920291add.htm).

We are most grateful to Alex Webb for his help with the ATP measurements, and to Steve Tovey for help with the FlexStation™ experiments. We also thank Gary Bird for the gift of HEK cells stably transfected with ER-targeted GFP, and Sarino Rizzuto, Colin Taylor and members of the Irvine laboratory for helpful discussions. D.B. was supported by the Wellcome Trust, and M.J.S. and R.F.I. were supported by the Royal Society.

REFERENCES

1 Rizzuto, R., Pinton, P., Brini, M., Chiesa, A., Filippin, L. and Pozzan, T. (1999) Mitochondria as biosensors of calcium microdomains. Cell Calcium **26**, 193–199
2 Malli, R., Frieden, M., Osibow, K., Zoratti, C., Mayer, M., Demaurex, N. and Graier, W. F. (2003) Sustained Ca^{2+} transfer across mitochondria is essential for mitochondrial Ca^{2+} buffering, store-operated Ca^{2+} entry, and Ca^{2+} store refilling. J. Biol. Chem. **278**, 44769–44779
3 Tinel, H., Cancela, J. M., Mogami, H., Gerasimenko, J. V., Gerasimenko, O. V., Tepikin, A. V. and Petersen, O. H. (1999) Active mitochondria surrounding the pancreatic acinar granule region prevent spreading of inositol trisphosphate-evoked local cytosolic Ca^{2+} signals. EMBO J. **18**, 4999–5008
4 Collins, T. J., Lipp, P., Berridge, M. J. and Bootman, M. D. (2001) Mitochondrial Ca^{2+} uptake depends on the spatial and temporal profile of cytosolic Ca^{2+} signals. J. Biol. Chem. **276**, 26411–26420
5 Csordas, G., Thomas, A. P. and Hajnoczky, G. (1999) Quasi-synaptic calcium signal transmission between endoplasmic reticulum and mitochondria. EMBO J. **18**, 96–108
6 Rintoul, G. L., Filiano, A. J., Brocard, J. B., Kress, G. J. and Reynolds, I. J. (2003) Glutamate decreases mitochondrial size and movement in primary forebrain neurons. J. Neurosci. **23**, 7881–7888
7 Yi, M., Weaver, D. and Hajnoczky, G. (2004) Control of mitochondrial motility and distribution by the calcium signal: a homeostatic circuit. J. Cell Biol. **167**, 661–672
8 Terasaki, M., Chen, L. B. and Fujiwara, K. (1986) Microtubules and the endoplasmic reticulum are highly interdependent structures. J. Cell Biol. **103**, 1557–1568
9 Lee, C. and Chen, L. B. (1988) Dynamic behavior of endoplasmic reticulum in living cells. Cell **54**, 37–46
10 Waterman-Storer, C. M. and Salmon, E. D. (1998) Endoplasmic reticulum membrane tubules are distributed by microtubules in living cells using three distinct mechanisms. Curr. Biol. **8**, 798–806
11 Yaffe, M. P. (1999) The machinery of mitochondrial inheritance and behavior. Science **283**, 1493–1497
12 Welte, M. A. (2004) Bidirectional transport along microtubules. Curr. Biol. **14**, R525–R537
13 Reynolds, I. J. and Rintoul, G. L. (2004) Mitochondrial stop and go: signals that regulate organelle movement. Science STKE **2004**, PE46
14 Overly, C. C., Rieff, H. I. and Hollenbeck, P. J. (1996) Organelle motility and metabolism in axons vs. dendrites of cultured hippocampal neurons. J. Cell Sci. **109**, 971–980
15 Pedrosa Ribeiro, C. M., McKay, R. R., Hosoki, E., Bird, G. S. and Putney, Jr, J. W. (2000) Effects of elevated cytoplasmic calcium and protein kinase C on endoplasmic reticulum structure and function in HEK293 cells. Cell Calcium **27**, 175–185
16 Bootman, M. D. and Berridge, M. J. (1996) Subcellular Ca^{2+} signals underlying waves and graded responses in HeLa cells. Curr. Biol. **6**, 855–865
17 Bird, G. S. and Putney, J. W. (2005) Capacitative calcium entry supports calcium oscillations in Human Embryonic Kidney Cells. J. Physiol. **562**, 697–706
18 Xia, Z., Dudek, H., Miranti, C. K. and Greenberg, M. E. (1996) Calcium influx via the NMDA receptor induces immediate early gene transcription by a MAP kinase/ERK-dependent mechanism. J. Neurosci. **16**, 5425–5436
19 Groskreutz, D. J., Sherf, B. A., Wood, K. V. and Schenborn, E. T. (1995) Increased expression and convenience with the new pGL3 luciferase reporter vectors. Promega Notes Magazine **50**, 2
20 Jouaville, L. S., Pinton, P., Bastianutto, C., Rutter, G. A. and Rizzuto, R. (1999) Regulation of mitochondrial ATP synthesis by calcium: evidence for a long-term metabolic priming. Proc. Natl. Acad. Sci. U.S.A. **96**, 13807–13812
21 Koop, A. and Cobbold, P. H. (1993) Continuous bioluminescent monitoring of cytoplasmic ATP in single isolated rat hepatocytes during metabolic poisoning. Biochem. J. **295**, 165–170
22 Allue, I., Gandelman, O., Dementieva, E., Ugarova, N. and Cobbold, P. (1996) Evidence for rapid consumption of millimolar concentrations of cytoplasmic ATP during rigor-contracture of metabolically compromised single cardiomyocytes. Biochem. J. **319**, 463–469
23 Mallik, R. and Gross, S. P. (2004) Molecular motors: strategies to get along. Curr. Biol. **14**, R971–R982
24 Carafoli, E. and Brini, M. (2000) Calcium pumps: structural basis for and mechanism of calcium transmembrane transport. Curr. Opin. Chem. Biol. **4**, 152–161
25 Hajnoczky, G., Robb-Gaspers, L. D., Seitz, M. B. and Thomas, A. P. (1995) Decoding of cytosolic calcium oscillations in the mitochondria. Cell **82**, 415–424
26 Ligon, L. A. and Steward, O. (2000) Movement of mitochondria in the axons and dendrites of cultured hippocampal neurons. J. Comp. Neurol. **427**, 340–350
27 Morris, R. L. and Hollenbeck, P. J. (1993) The regulation of bidirectional mitochondrial transport is co-ordinated with axonal outgrowth. J. Cell Sci. **104**, 917–927
28 Li, Z., Okamoto, K., Hayashi, Y. and Sheng, M. (2004) The importance of dendritic mitochondria in the morphogenesis and plasticity of spines and synapses. Cell **119**, 873–887

Received 4 May 2005/17 June 2005; accepted 28 June 2005
Published as BJ Immediate Publication 28 June 2005, doi:10.1042/BJ20050738